Korean J. Chem. Eng., 36(10), 1575-1586 (2019)
DOI: 10.1007/s11814-019-0356-1

pISSN: 0256-1115
eISSN: 1975-7220

Removal of crystal violet dye by an efficient and low cost adsorbent: Modeling, kinetic, equilibrium and thermodynamic studies

Maliheh Sarabadan*, Hadis Bashiri*,†, and Seyed Mahdi Mousavi**

*Department of Physical Chemistry, Faculty of Chemistry, University of Kashan, Kashan, Iran
**Department of Applied Chemistry, Faculty of Chemistry, University of Kashan, Kashan, Iran
(*Received 19 December 2018 • accepted 8 August 2019*)

Abstract−Natural zeolite as a low cost clay was tested for removal of crystal violet known as a noxious dye. Five characterization techniques were used for this study. Optimizing and modeling of adsorption were performed at minimum time by an applicable technique named as response surface methodology (RSM). Three effective variables (pH, temperature (T) and adsorbate-to-adsorbent ratio (a/A)) were monitored to obtain the dye removal efficiencies. The maximum removal of dye was obtained at pH=10, T=25 °C and a/A=0.1 g/g. For natural zeolite, the Fractal-Langmuir model was selected as an appropriate model for kinetic studies and the Freundlich isotherm was the best isotherm for equilibrium studies. Thermodynamic investigations showed that the adsorption of dye on natural zeolite is endothermic process and a spontaneous reaction. The maximum dye adsorption capacity of natural zeolite and Merck activated carbon on the surface of each adsorbent was obtained at 177.75 and 84.11 mg/g, respectively. In comparison with the maximum adsorption capacity of activated carbon obtained from Merck Company, we can conclude that natural zeolite possesses a higher adsorption capacity. These results reveal that, natural zeolite is an excellent and affordable adsorbent for removal of crystal violet from wastewater as compared to activated carbon.

Keywords: Adsorption, Natural Zeolite, Response Surface Methodology, Optimization, Kinetics, Dye Removal

INTRODUCTION

One of the main environmental issues is the quality of water and drinking water. Many of the water sources are contaminated by dyes. Dyes are basically complicated molecules that are very difficult to degrade naturally in the water system. They are noxious, carcinogenic and very hazardous. Crystal violet (CV) as a cationic dye is toxic and very dangerous [1,2]. It leads to respiratory failure, brain confusion and eye irritation. This dye is used in textile, paper and wood industries, veterinary medicine and drugs [3,4]. Hence, the removal of this dye from environment is critical and essential. For increasing water quality, several ways have been investigated [5,6]. Adsorption methods are widely applicable because they are fast and require lower cost [7,8].

Some economic and effective adsorbents are used for removal of dyes, such as activated slag [9], fly ash [10] and zeolites [11]. Zeolites are extensively used as adsorbents in environmental systems because of their porous structure, high adsorption capacity, low cost, non-toxicity and abundance in nature. The adsorption of CV on the zeolite occurs by electrostatic attraction between the negatively charged sites of the adsorbent and the positively charged dye molecules and also by cation exchange. Zeolites have various structures which consist of a three-dimensional network with a negative charge balanced by some cations such as Na^+, K^+, Mg^{2+} and Ca^{2+} [12]. These cations can be exchanged with some cations in water [13-15]. Ability of zeolites to remove several cationic dyes such as methylene blue, safranine and malachite green and so on has been proved [16], while adsorption studies of anionic dyes are very limited. Zeolites have narrow pores, which makes access difficult for some dye molecules [17]. The pore size of clinoptilolite has the largest maximum dimensions (0.76 nm) of the zeolites studied [18]. Therefore, the size of cationic dyes is an important factor in ion-exchange mechanism and zeolites have more affinity for the dyes with the small molecular size [16]. The molecular dimension of the dyes affects the adsorption capacity and the adsorption rate. The molecular dimension (°A) of CV is 11.37×10.25×8.70 [19]; this study will show it can penetrate into the pores of natural zeolite or not.

Activated carbons are used as suitable adsorbents in removal of pollutants from wastewater. They have high adsorption capacity and can adsorb both cationic and anionic dyes [20,21]. Merck activated carbon is one of the best adsorbents for dye removal since it has high adsorption capacity, but it is expensive [8,22]. For example, adsorption of dyes (methylene blue (MB) and methyl orange (MO)) on activated carbon prepared from apricot stones and commercial activated carbon was investigated by Djilani et al [23]. They prepared an activated carbon from apricot stones and compared it to a commercial activated carbon. The maximum uptake of MB and MO onto two activated carbons under optimized conditions was determined to be 99.5%. Belaid et al. [24] investigated adsorption kinetics of some textile dyes onto granular activated carbon. They showed that the Elovich model describes the experimental results, and adsorption process of dyes onto heterogeneous surface of activated carbon is chemisorption. Giannakoudakis et al. investigated multi-parametric adsorption effects of the reactive dye removal with

†To whom correspondence should be addressed.
E-mail: hbashiri@kashanu.ac.ir, h.bashiri@ymail.com

commercial activated carbons. They used three commercial carbons (DARCO, R008, PK13) for removal of RB5 from aqueous solutions. Equilibrium experiments was performed by using Langmuir, Freundlich and Langmuir-Freundlich isotherms and the maximum adsorption capacity for all carbon samples at 25 °C was 348, 527, 394 mg/g for DARCO, R008, PK13, respectively [25]. Yavuz et al. [26] investigated removal of direct dyes (direct yellow, direct red and direct blue) from an aqueous solution by different adsorbents such as activated carbon, raw kaolinite and montmorillonite. They showed that commercial activated carbon has the highest removal efficiency and adsorption capacity among other adsorbents.

In this study, we performed the adsorption of CV onto natural zeolite and Merck activated carbon and compared the obtained results. This comparison shows that some natural adsorbents such as natural zeolite can have high adsorption capacity like some expensive and high efficiency adsorbents such as Merck activated carbon. Some variables can affect the response of an adsorption experiment and they can be optimized and modeled to obtain maximum of efficiency. Response surface methodology (RSM) helps to investigate the effective variables to design experiments and obtain optimum conditions at less times [27,28]. For example, Karimifard and Alavi Moghaddam optimized removal of Reactive Blue using carbon nanotubes by RSM [29]. Satapathy et al. investigated the adsorption process of crystal violet using a novel nanocomposite by RSM [30].

In this paper, removal of CV by natural zeolite and modeling of adsorption process was studied. The zeolite used in this study is not expensive and is abundant in nature. The important variables for CV adsorption on this zeolite were examined by RSM. Also, the kinetics, isotherms and thermodynamic studies were performed. The maximum adsorption capacity of this adsorbent at optimum condition was compared with activated carbon from Merck Company and various adsorbents. It was shown that natural adsorbents such as zeolite can be comparable with the synthesized or commercial adsorbents such as Merck activated carbon.

EXPERIMENTAL

1. Materials

Natural zeolite was collected from Semnan city in Iran. The size of sample particles ranged from μm to nm. For purification of collected samples, 20 g of zeolite was initially dispersed in 600 mL deionized water and placed in a shaker at 130 rpm for 24 h. Then, the mixture was filtered and zeolite was washed with deionized water and dried into oven at 120 °C for 12 h. Crystal violet ($C_{25}H_{30}N_3Cl$) and activated carbon were procured from Merck company and were used without further purification. A solution of CV with concentration 1,000 mg/L was prepared by dissolving 1.00 g of CV in 1 L deionized water. The HCl and NaOH solutions (0.1 N) were purchased from Merck Company.

2. Instrumentation

Chemical functional groups were identified by Fourier transform infrared (FTIR) absorption spectra, which were obtained with an infrared spectrophotometer with the KBr pellet technique (FTIR-Magna 550 - Nicolet). The structure was investigated by powder X-ray diffraction (XRD) patterns of the as-prepared samples which were recorded on the X-ray diffractometer (XRD, Philips X" pert Pro MPD) using Cu kα X-ray irradiation. Specific surface area was determined using surface area analyzer (BEL Sorb Gas Adsorption Analyzer). Morphology was revealed by field emission scanning electron microscopy (FE-SEM) and was performed by electron microscope (MIRA3 TESCAN). The absorbance spectra were obtained using UV-Vis spectrophotometer (Shimadzu Model: T-80).

3. Experimental Design

Experimental design enables researchers to obtain useful information concerning the effect of various variables on the response. Central composite design (CCD) was used to consider the importance of variables on the removal efficiency of CV [31]. In this work, dye removal efficiency (%) by the natural zeolite was studied using CCD with α=±1.68. The selected variables were pH (3-11), temperature (25-55 °C) and adsorbate-to-adsorbent (a/A) weight ratio (0.1-0.5 g/g). Design Expert software (Ver. 8.0.7.1) was used and 20 experiments were designed and recorded in Table 1. The correlation between the response and the selected variables can be expressed by:

$$y = \beta_0 + \Sigma_{i=1}^{3}\beta_i x_i + \Sigma_{i=1}^{3}\beta_{ii} x_i^2 + \Sigma_{i=1}^{2}\Sigma_{j=i+1}^{3}\beta_{ij} x_i x_j + \varepsilon \quad (1)$$

where, β_0 is a constant term, β_i is the linear effect term, β_{ii} is the quadratic effect term, and β_{ij} is the interaction effect term; x_i and x_j are factors; ε is the residue and y is the response.

4. Adsorption Experiments

To perform the equilibrium studies of CV adsorption on natural zeolite, 50 mL of the CV solutions with different concentrations (20-200 mg/L) were mixed with 2 g/L of natural zeolite and then put for 24 h in a shaker (130 rpm). The equilibrium experiment for CV adsorption on activated carbon was performed by mixing

Table 1. The CCD matrix and value of CV removal efficiency

Run	pH	Temperature (°C)	Adsorbate-to-adsorbent weight ratio (g/g)	Removal efficiency (%)
1	7	40	0.3	93.6
2	9.38	31.08	0.42	93.85
3	7	40	0.3	94.01
4	4.62	31.08	0.42	90.21
5	9.38	31.08	0.18	97.22
6	4.62	48.92	0.42	90.7
7	4.62	48.92	0.18	97.36
8	7	40.00	0.30	94.1
9	11	40	0.3	98
10	9.38	48.92	0.18	98.1
11	7	40	0.3	93.1
12	7	40	0.1	96.9
13	7	40	0.3	95.1
14	7	40	0.3	93.7
15	3	40	0.3	90.7
16	7	55	0.3	97.76
17	7	40	0.5	90.21
18	4.62	31	0.18	94.6
19	7	25	0.3	94.01
20	9.38	48.92	0.42	97.1

1 g/L of Merck carbon with 50 mL of the CV solution (30, 40, 50, 60, 70 and 80 mg/L), and solutions were put for 24 h in a shaker (130 rpm). After equilibrium, the CV concentrations were determined using the UV-visible spectrophotometer at λ_{max}=590 nm. The removal percentage of CV is representing by Eq. (2):

$$R\% = \frac{C_0 - C_e}{C_0} \times 100 \quad (2)$$

where, C_0 and C_e are the initial and equilibrium concentrations of CV (mg/L), respectively. The amount of adsorbed CV at equilibrium can be expressed by:

$$q_e = \frac{(C_0 - C_e)V}{W} \quad (3)$$

where, V (mL) is the volume of CV solution and W (g) is the weight of zeolite or activated carbon.

For studying the adsorption kinetic, 50 mL of CV solutions (4, 6, 8, 10 mg/L) was added to 2 g/L of the natural zeolite, and then the solutions were placed in a shaker with 130 rpm. The CV concentrations in the solutions were determined at different adsorbing times (2-300 min) and the amount of adsorbed CV at each time was obtained by:

$$q = \frac{(C_0 - C_t)V}{W} \quad (4)$$

where, C_t (mg/L) is the concentration of CV after the corresponding adsorption time and V (mL) and W (g) are the volume of CV solution and the weight of zeolite and activated carbon, respectively.

RESULTS

1. Characterization

XRD, FT-IR, BET, FE-SEM and EDX were performed to analyze the chemical composition and morphology of natural zeolite. The XRD pattern of natural zeolite shows clinoptilolite is the main component with minor amounts of gypsum and quartz (Fig. 1(a)). The reflections in pattern referred to the presence of various forms of clinoptilolite (2θ=10°, 12°) with chemical formula of (Na, K,

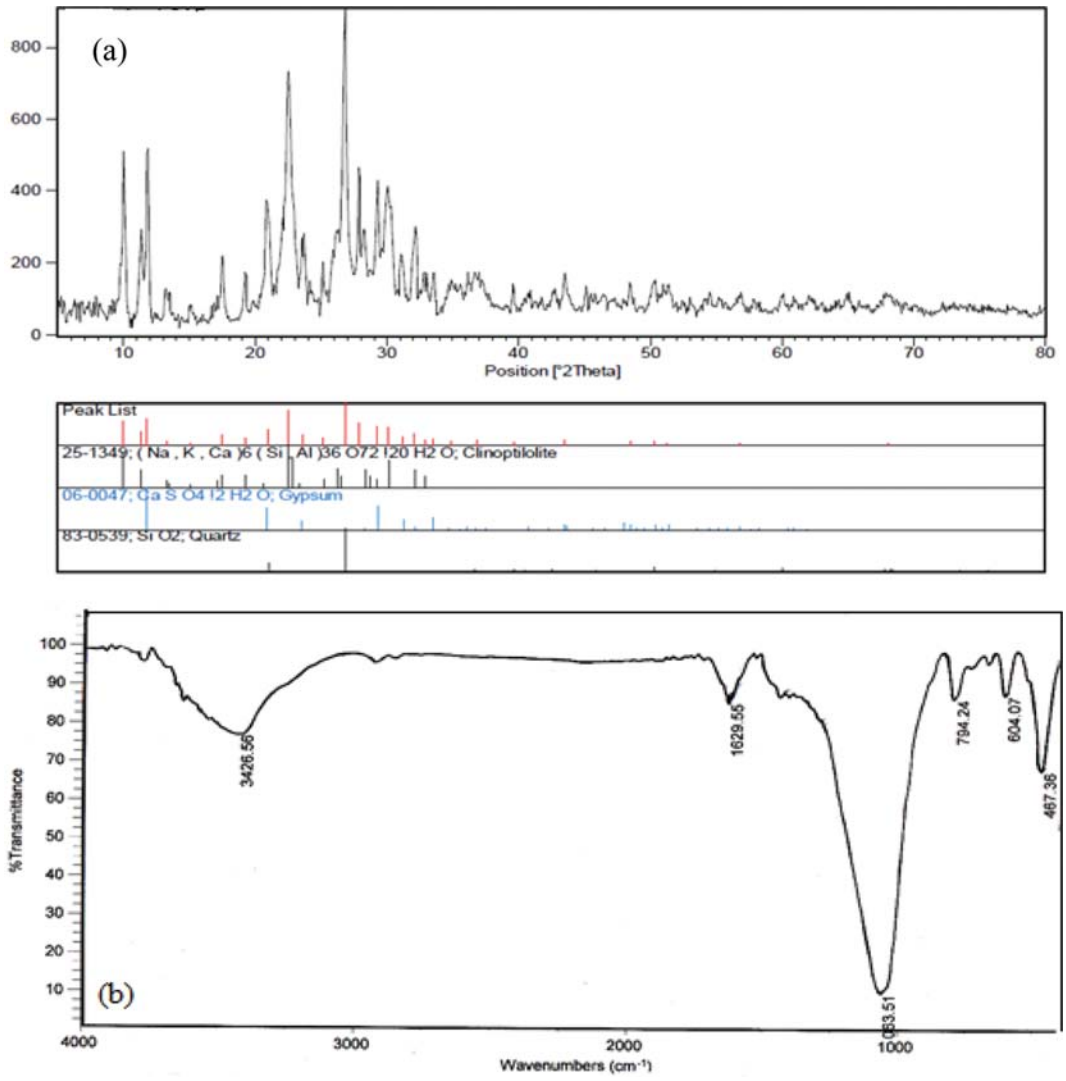

Fig. 1. The XRD (a) and FT-IR (b) spectra for natural zeolite.

$Ca)_6(Si, Al)_{36}O_{72}\cdot 20\ H_2O$, gypsum ($2\theta$=22.5°) with chemical formula of $CaSO_4\cdot 2H_2O$ and quartz (SiO_2) at 2θ=27.5° [32]. Zeolites generally display an affinity for cationic dyes like CV. The adsorption of CV on the zeolite occurs by electrostatic attraction between adsorbent and dye molecules and also by cation exchange. The size of dye and the pore size of zeolite are important variables in the dye adsorption process by zeolites. The pore size of clinoptilolite has the dimensions 0.76 nm [18]. GaussView software was used to calculate molecular size of CV. It was obtained as 9.72 °A and with respect to its size, it cannot penetrate into the pores of zeolite.

In the FT-IR spectrum of natural zeolite, the bands located at 400-1,200 cm^{-1} wavelength are attributed to the vibrations of the Si-O-Si and Si-O-Al [33]. The most intense bands at 1,063, 1,629, and 3,426 cm^{-1} can be assigned to external tetrahedral linkage asymmetric stretching, stretching vibration mode of adsorbed water in natural zeolite, and intermolecular hydrogen bonding, respectively (Fig. 1(b)).

The BET surface area of natural zeolite corresponds to 24.08 m^2/g and pore volume was determined as 0.1130 cm^3/g; additionally, its mean pore diameter is equal to 18.761 nm. It seems that zeolite particles are aggregated or some big zeolite particles have holes so that some big mesopores of 18.761 nm are created.

The FE-SEM images of natural zeolite in magnifications: (a) 2 μm, (b) 1 μm and (c) 500 nm are shown in Fig. 2. These images show the surface texture and porosity and also, the particle size and cavity shape of natural zeolite. The SEM images show that zeolite particles are aggregated and some big mesopores are created in the adsorbent samples. The CV molecules can be adsorbed on the outer surface of smaller zeolite particles or the holes of big zeolite particles not inside the zeolites.

EDX micrograph shows that the Si compounds are the major portion of natural zeolite, so they are suitable for the adsorption of organic dyes such as CV. The weight percent (wt%) of O, Si, Al, K, Na, Fe and Mg compounds within the adsorbent was determined as 55.62, 33.3, 5.40, 3.12, 1.65, 0.62 and 0.2%, respectively (Fig. 3).

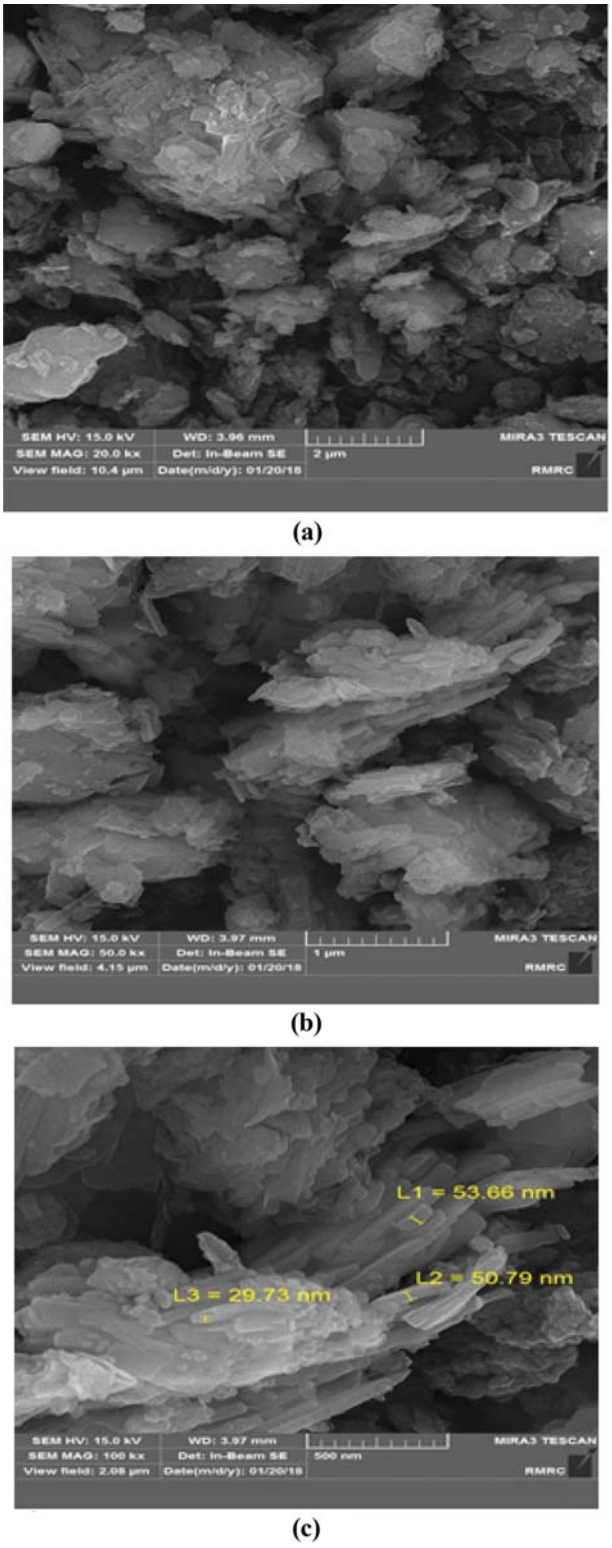

Fig. 2. The FE- SEM images of natural zeolite in different magnification: (a) 2 μm, (b) 1 μm and (c) 500 nm.

2. Response Surface Methodology

2-1. Regression Model Equation

According to the results, a second-order polynomial equation was obtained [34]. The correlation between response, R, and independent variables is:

$$R=+93.93+1.88\times A+1.00\times B-1.95\times C+0.11\times A\times B +0.84\times A\times C+0.013\times B\times C+0.2\times A^2+0.74\times B^2-0.08\times C^2 \quad (5)$$

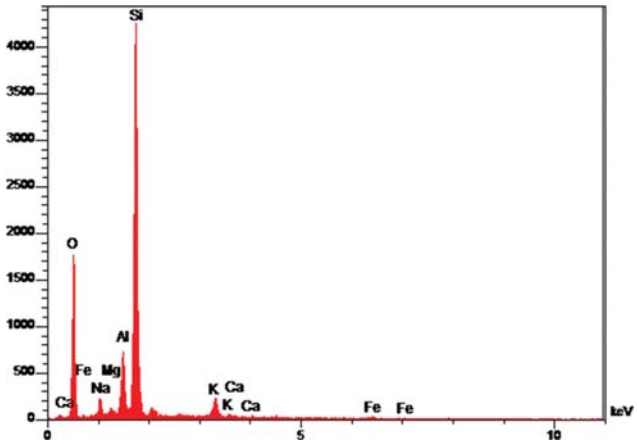

Fig. 3. The EDX micrograph of natural zeolite.

Table 2. ANOVA analysis for the fit of the experimental data to response surface model

Source	Sum of squares	DF	Mean square	F-value	P-value prob. >
Model	128.36	9	14.26	23.37	<0.0001
A-pH	48.28	1	48.28	79.11	<0.0001
B-temp	13.72	1	13.72	22.48	0.0008
C-wt%	52.09	1	52.09	85.35	<0.0001
AB	0.097	1	0.097	0.16	0.6988
AC	5.58	1	5.58	9.14	0.0128
BC	0.0012	1	0.0012	0.0020	0.9648
A^2	0.58	1	0.58	0.95	0.3525
B^2	7.96	1	7.96	13.05	0.0047
C^2	0.093	1	0.093	0.15	0.7042
Residual	6.10	10	0.61		
Lack of fit	3.85	5	0.77	1.71	0.2859
Pure error	2.25	5	0.45		
Cor total	134.46	19			
Model statistics summary					
Std. Dev	0.78		R-Squared		0.9546
C.V	0.83		Adj R-Squared		0.9138
Adeq. precision	17.507		Pred R-Squared		0.7271

In this equation, pH, temperature and adsorbate-to-adsorbent weight ratio are denoted by A, B and C, respectively. Hence, pH and temperature have a positive effect on the dye removal and by their increasing, the dye removal increases. The adsorbate-to-adsorbent weight ratio has a negative effect on the dye removal, and by increasing of this ratio, the dye removal decreases.

2-2. Analysis of Variance (ANOVA)

The ANOVA results help identify the role and importance of each variable and also the accuracy of the selected model [35]. Low *P*-value of 0.0001, high *F*-value of 23.37, high R^2 of 0.9546 and insignificant lack of fit reveal that the model is accurate (Table 2). The results reveal the adsorbate-to-adsorbent weight ratio is the most effective variable and temperature is the least effective variable. The lack of fit *F*-value 1.71 implies that it is not significant relative to the pure error. Adequate precision measures the signal-to-noise ratio, and adequate precision of 17.507 reveals that this model can be applied for design space navigation.

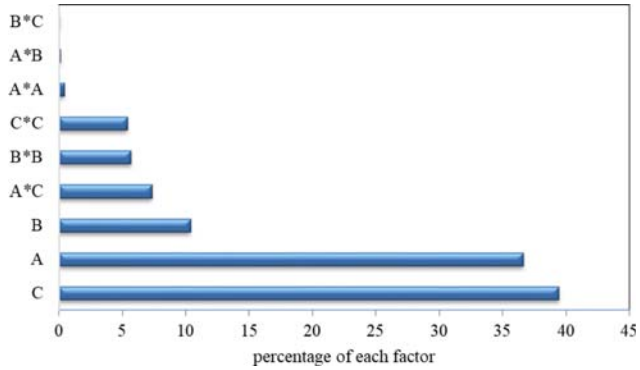

Fig. 4. Pareto graphic analysis for CV removal.

A Pareto analysis indicates the percentage effect of each variable on the dye removal efficiency. The results of the Pareto analysis show that adsorbate-to-adsorbent weight ratio is the most effective variable in dye removal (Fig. 4).

2-3. CCD Plots

A perturbation plot helps to compare the effect of all the variables at a special point in the design space [36]. This plot shows that pH and temperature have positive effects, while adsorbate-to-adsorbent weight ratio indicates a negative effect on the dye removal efficiency (Fig. 5).

The surface plots from the model help to indicate the effect of the interactions of variables on dye removal (Fig. 6). In Fig. 6, pH

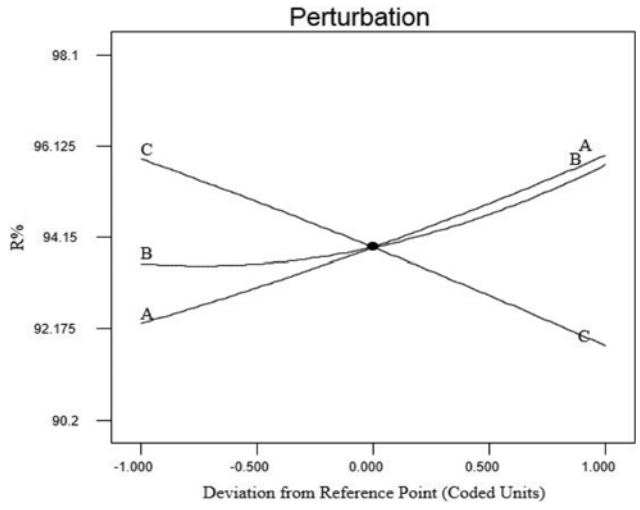

Fig. 5. The perturbation plots: pH (A), temperature (B), adsorbate-to-adsorbent weight ratio (C) and dye removal efficiency (R%).

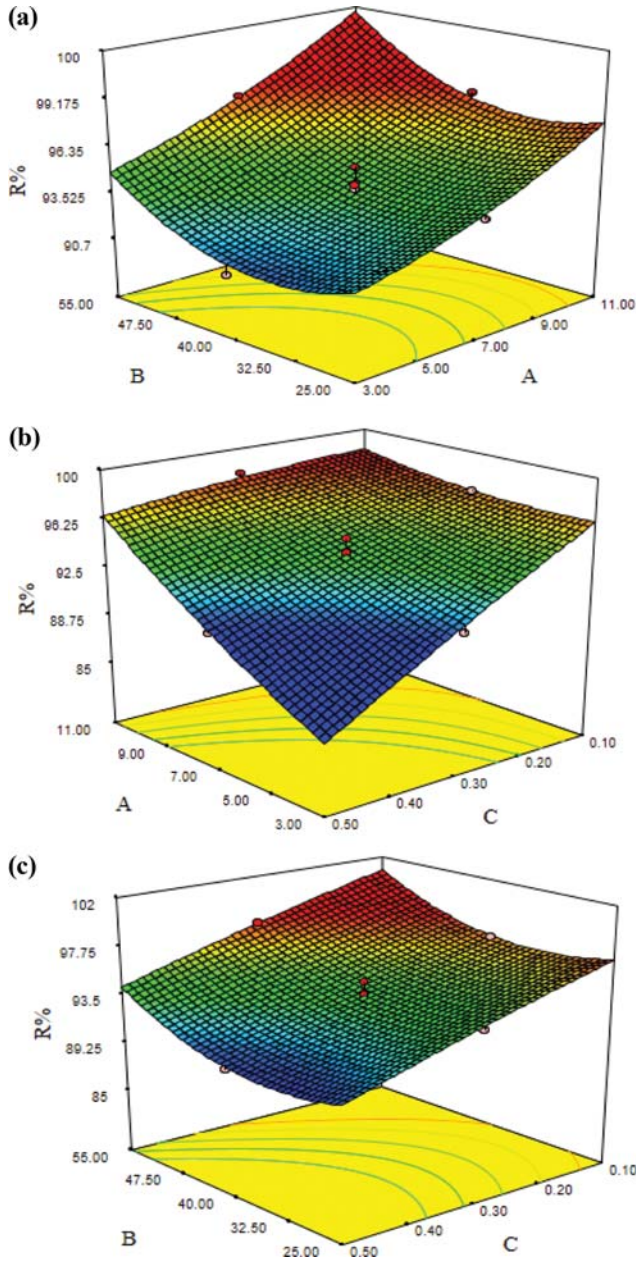

Fig. 6. Response surface and counter plots: pH (A), temperature (B), adsorbate-to-adsorbent weight ratio (C) and dye removal efficiency (R%).

is labeled A, temperature is labeled B and adsorbate-to-adsorbent weight ratio is labeled (C), respectively. The effect of pH and temperature on the efficiency of CV removal reveals the efficiency of removal increases with pH increasing (Fig. 6(a)). It is because at high pH there is an excessive number of negative sites on the zeolite surface, which leads to adsorption of cationic dye. The influence of pH and adsorbate-to-adsorbent weight ratio indicates that the efficiency of dye removal decreases at high weight ratio of adsorbate to adsorbent, because at high concentration of adsorbate, many of the adsorbent sites are covered, while at lower dye concentration, most of the sites are uncovered (Fig. 6(b)). The interaction between temperature and adsorbate-to-adsorbent weight ratio indicates that

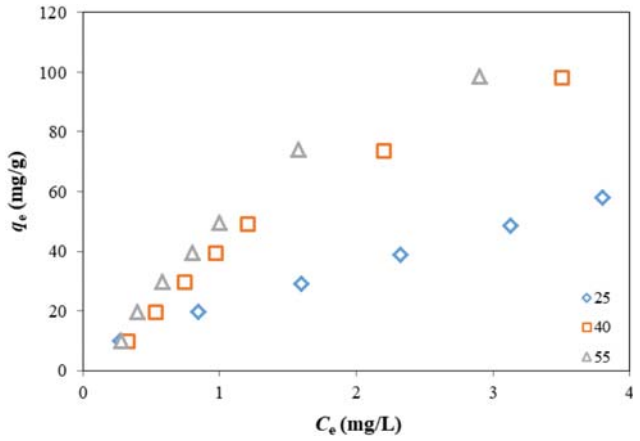

Fig. 7. Adsorption isotherms of CV on natural zeolite at different temperature (25, 40, 55 °C).

the removal of CV is facilitated by temperature increasing. With increasing temperature, the mobility of dye molecules increases and it facilitates their adsorption on the surface (Fig. 6(c)).

2-4. Optimization Study

To determine the optimum conditions for maximum of dye removal, variables of adsorbate-to-adsorbent weight ratio (a/A), temperature and pH were set in the studied range. Design Expert software suggested 0.1 g/g of adsorbate-to-adsorbent weight ratio (a/A), temperature 25 °C and pH of 10 as the optimum conditions to achieve the maximum dye removal efficiency of 99.9%.

3. Effect of Temperature of Solution

Fig. 7 shows the adsorption isotherms of CV on natural zeolite at different temperatures (25-55 °C). This Figure shows the q_e value at 55 °C (74.2 mg/g) is higher than that at 25 °C (72.4 mg/g). By temperature increasing, the mobility of dye ions in solution will increase and interaction between dye ions with active sites on the surface of adsorbent will increase. At high temperature, large dye molecules can penetrate into the pores of zeolite. Also, the adsorption capacity increases by temperature increasing, which indicates the endothermic nature of adsorption process.

4. Adsorption Isotherm

Equilibrium studies for CV adsorption on natural zeolite were carried out by mixing 2 g/L of clay with various concentrations of CV (20, 40, 60, 80, 100 and 200 mg/L) at the optimum values of pH and temperature. The equilibrium experiment for CV adsorption on activated carbon was carried by mixing 1 g/L of Merck carbon with 50 mL of the CV solution (30, 40, 50, 60, 70 and 80 mg/L) and solutions were placed during 24 h in a shaker (130 rpm). After equilibrium, concentrations of CV in solutions were analyzed. Adsorption isotherms were investigated to evaluate the maximum adsorption capacities of these two adsorbents. Fig. 8(a) shows the adsorption isotherm of CV on natural zeolite. Fig. 8(b) shows the adsorption isotherm of CV on activated carbon from Merck company. Applied concentration ranges for CV adsorption on zeolite and activated carbon were different. We investigated zeolite in optimum condition and, therefore, it was applied in large concentration range. Adsorption isotherms show at low concentration of CV, activated carbon works better than natural zeolite, and at high con-

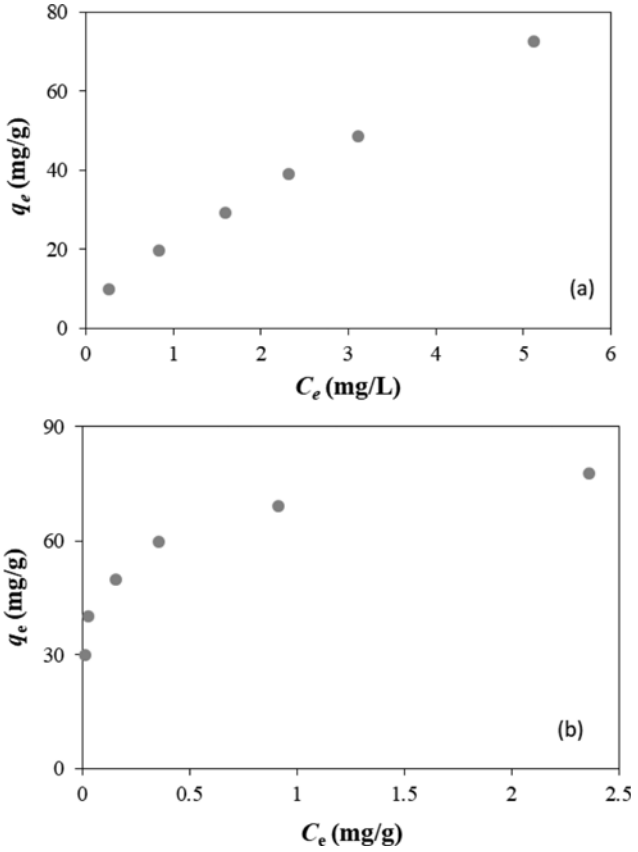

Fig. 8. Adsorption isotherm of CV on (a) natural zeolite (pH 10, temperature 25 °C, adsorbent dosage 2 g/L and initial dye concentrations 20-200 mg/L) and (b) activated carbon of Merck Company (pH 7, temperature 25 °C, adsorbent dosage1 g/L and initial dye concentrations 30-80 mg/L).

centration zeolite is a better adsorbent. Therefore, activated carbon can be used for low concentration of CV, while zeolite has higher adsorption capacity. The nonlinear fittings of isotherms for two adsorbents were performed by using Langmuir, Freundlich, Temkin, Redlich-Peterson, Sips and Flory-Huggins isotherms.

4-1. Langmuir Isotherm

Langmuir isotherm is applied for monolayer adsorption with the limited number of active sites which have similar situations [37]. The Langmuir isotherm is given as:

$$q_e = \frac{q_m K_L C_e}{1 + K_L C_e} \tag{6}$$

where, K_L is the Langmuir adsorption constant (L/mg) and q_m is the maximum adsorption capacity (mg /g). The obtained values of q_m, K_L and R^2 are presented in Table 3.

4-2. Freundlich Isotherm

For heterogeneous surfaces with a different distribution of heat of sorption over the surface, Freundlich isotherm is used [38]:

$$q_e = K_F C_e^{\frac{1}{n}} \tag{7}$$

where, K_F is the Freundlich adsorption constant and n is a constant related to the surface heterogeneity.

Table 3. Parameters for adsorption isotherms on natural zeolite and Merck activated carbon

Models	Parameter	Natural zeolite	Merck activated carbon
Langmuir isotherm	q_{max} (mg/g)	106.67	67.09
	K_L (L/mg)	0.266	47.52
	R^2	0.9604	0.8574
Freundlich isotherm	K_f (L/mg)	21.99	70.23
	n	1.5	5.0
	R^2	0.9946	0.9781
Redlich-Peterson isotherm	A (L/g)	6468	6309
	B (L/mg)	286.70	90.20
	g (L/mg)	0.33	0.87
	R^2	0.9939	0.9893
Temkin isotherm	B_1 (J·g/mol·mg)	13.57	31.54
	A_1 (L/mg)	7.5371	10.75
	R^2	0.8307	0.9783
Sips isotherm	q_{max} (mg/g)	175.54	84.11
	K_{LF} (L/mg)	0.0904	22.76
	n	1.240	1.6
	R^2	0.9786	0.9994
Flory-Huggins isotherm	q_{max} (mg/g)	177.75	91.48
	$K_{F\text{-}H}$	20.54	34.14
	n	1.22	2.67
	R^2	0.9832	0.9785

4-3. Temkin Isotherm

Temkin and Pyzhev [39] investigated the effects of adsorbate-adsorbate interactions, and they assumed that the heat of adsorption of all the molecules because of these interactions would decrease linearly with coverage. Temkin isotherm has the following form:

$$q_e = B_T \ln K_T + B_T \ln C_e \tag{8}$$

where, B_T is a temperature dependent constant related to the heat of adsorption and K_T is the equilibrium constant (L/mg).

4-4. Redlich-Peterson Isotherm

Redlich-Peterson model, which investigates three parameters in an isotherm, is used for both monolayer and multilayer adsorption [40]:

$$q_e = \frac{AC_e}{1 + BC_e^g} \tag{9}$$

where A, B and g are the constants, and $0<g<1$.

4-5. Sips (Langmuir-Freundlich) Isotherm

Sips or Langmuir-Freundlich isotherm assumes that adsorbent surface is heterogeneous, and it has different distribution of heat of sorption [41]:

$$q_e = q_m \frac{(K_{LF} C_e)^{1/n}}{1 + (K_{LF} C_e)^{1/n}} \tag{10}$$

where K_{LF} is Langmuir-Freundlich constant (L/mg) and n is a non-dimensional parameter for surface heterogeneity.

Table 4. Maximum adsorption capacities of CV obtained by different adsorbents

Adsorbent	Maximum adsorption capacity (mg/g)	References
Magnetic carbon-iron oxide nanocomposite	81.7	[44]
Soil-Ag NP	1.918	[30]
ZnO-NRs-AC	113.64	[46]
Semi-IPN hydrogels	35.09	[2]
Magnetic Zeolite	0.9711	[47]
Almond Shell	114	[68]
Zeolite from fly ash	19.6	[45]
Zeolite from bottom ash	17.6	[45]
Amino silica	40	[50]
Kaolin	47.27	[49]
Polyacrylamide-bentonite composite	144.60	[51]
Kaolinite-supported zero-valent iron	129.9	[52]
Phosphoric acid activated carbon	60.42	[48]
Sulfuric acid activated carbon	85.84	[48]
Magnetically modified activated carbon	67.1	[53]
$SnFe_2O_4$@activated carbon magnetic nanocomposite	158.73	[54]
Natural zeolite	177.75	This work
Merck activated carbon	84.11	This work

4-6. Flory-Huggins Isotherm

The Flory-Huggins (FH) isotherm can be used for an adsorbent with several geometries of adsorption on the surface:

$$q_e = \frac{C_e(q_m - q_e)^n}{K_{FH}} \quad (11)$$

where, K_{FH} is Flory-Huggins constant.

All isotherm equations were fitted with experimental data, and the results of fittings with isotherms and the values of their corresponding correlation coefficients (R^2) are listed in Table 3. For CV adsorption on natural zeolite, the Freundlich isotherm is the best. Therefore, the adsorption process is non-ideal, reversible and not restricted to the formation of monolayer. Dye adsorption onto adsorbent can be multilayer, with non-uniform distribution of adsorption heat and affinities over the heterogeneous surface. A favorable adsorption tends to having the Freundlich constant n between 1 and 10. Larger value of n implies stronger interaction between adsorbent and dye, while 1/n equal to 1 indicates linear adsorption leading to identical adsorption energies for all sites [42]. In this study, n value was obtained as 1.5; therefore, the interaction between natural zeolite and CV is not strong and its surface heterogeneity is not high.

For Merck activated carbon, the Sips or Langmuir-Freundlich isotherm is the best. It can be assumed the adsorbent surface is heterogeneous and the adsorption process is monolayer. Sips isotherm circumvents the limitation of the rising adsorbate concentration associated with the Freundlich isotherm. At low adsorbate concentrations, it reduces to the Freundlich isotherm; while at high concentrations, it predicts a monolayer adsorption capacity characteristic of the Langmuir isotherm [43]. In the Sips isotherm, n is a parameter for surface heterogeneity. Different models are suitable for these adsorbents, because the surfaces of zeolite and activated carbon are different from each other. The maximum adsorption capacity of natural zeolite at optimum condition and activated carbon was obtained 177.75 mg/g and 84.11 mg/g, respectively.

Table 4 presents the comparison of the maximum adsorption capacities of CV of natural zeolite at optimum condition with Merck activated carbon and some adsorbents [2,30,44-54]. It was revealed that the maximum adsorption capacity of natural zeolite (177.75 mg/g) is higher than Merck activated carbon and other adsorbents, while some of them can be hardly prepared and the most of them are more expensive than zeolite.

5. Adsorption Kinetic

Kinetic studies of CV adsorption onto the natural zeolite were carried out with 2 g/L of adsorbent at CV concentrations of 4, 6, 8, 10 mg/L, adsorption time of 2-300 min and at the optimum values of pH and temperature. The obtained results are shown in Fig. 9. In this study, the kinetics models pseudo-first-order (PFO), pseudo-second-order (PSO), Elovich, Modified pseudo-first-order (MPFO),

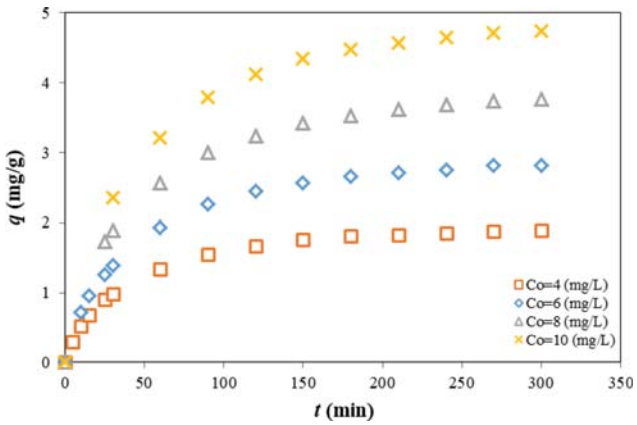

Fig. 9. Adsorption kinetics of CV on natural zeolite (pH 10, temperature 25 °C, adsorbent dosage 2 g/L and initial dye concentration 4, 6, 8, 10 mg/L).

intraparticle diffusion, integrated Kinetic Langmuir (IKL) and fractal like-integrated kinetic Langmuir (FLIKL) were investigated to study the adsorption kinetics. Linear regressions of kinetics models are broadly applied in the previous works. Recently, Simonin revealed mistakes using the linear fit for a nonlinear model [55]. He indicated a linear fit of *t*/*q* versus time always lead to a perfect linear fit, because of the linear increase of time over time, not because of the properties of the measured dependent variable q_t. The kinetic data were fitted by the nonlinear form of kinetic models.

5-1. Pseudo-first-order Model

Pseudo-first-order equation of Lagergren [56] is expressed as:

$$\frac{q}{q_e} = 1 - \exp(-k_1 t) \tag{12}$$

where, k_1 (min^{-1}) is the pseudo-first-order rate constant.

5-2. Pseudo-second-order Model

Pseudo-second-order model [57] is represented by following equation:

$$\frac{q}{q_e} = \frac{k_2^* t}{1 + k_2^* t} \tag{13}$$

where, k_2 is the pseudo-second-order rate constant.

5-3. Elovich Model

The Elovich is another rate equation [58], which is expressed as follows:

$$\frac{q}{q_e} = \frac{1}{\beta q_e}\ln(\alpha\beta) + \frac{1}{\beta q_e}\ln t \tag{14}$$

where, α is the initial adsorption rate and β is the relationship between the degree of surface coverage and the activation energy involved in the chemisorption.

5-4. Modified Pseudo-first-order Model

The modified-pseudo-first order (MPFO) kinetic equation proposed by Yang and Al-Duri simulates well the behavior of the kinetics governed by the rate of adsorption [59]. Then, it was obtained based on the statistical rate theory [60]:

$$\frac{q}{q_e} = \ln q_e - k_m t + \ln(q_e - q) \tag{15}$$

where, k_m is modified pseudo-first-order rate constant.

5-5. Intra Particle Diffusion Model

Generally, a process is diffusion-controlled if its rate depends on the rate at which components diffuse towards one another [61] and the adsorption rate can be expressed by:

$$q = k_i t^{\frac{1}{2}} + I \tag{16}$$

where, k_i is intraparticle diffusion rate constant.

5-6. Integrated Kinetic Langmuir Model

The kinetic Langmuir models had no analytical solutions until integrated kinetic Langmuir method was provided [62-64]. IKL is a simple and easy but complete method to obtain an analytical solution. It is expressed by Marczewski [64] for non-dissociative adsorption:

$$\frac{q}{q_e} = \frac{(1 - e^{-k_L t})}{(1 - a e^{-k_L t})} \tag{17}$$

where, a and k_L are IKL equation constants.

Table 5. Kinetic parameters for CV adsorption on natural zeolite

Models	Parameters	C_0 (mg/L)			
		4	6	8	10
Pseudo-first order	k_1 (min^{-1})	0.0223	0.0200	0.0188	0.0182
	R^2	0.9821	0.9816	0.9821	0.9912
Pseudo-second order	k_2 (mg g^{-1} min^{-1})	0.0216	0.0134	0.0106	0.0565
	R^2	0.9813	0.9760	0.9705	0.9664
Elovich	α (mg/g·min)	0.1606	0.2054	0.4861	0.4618
	β (g/mg)	2.4474	1.5840	1.2400	1.0260
	R^2	0.9121	0.9870	0.9781	0.9597
MPFO	k_M $(min)^{-1}$	0.0107	0.0104	0.0105	0.0115
	R^2	0.9743	0.9630	0.9617	0.9492
Intra particle diffusion	k_i	0.1048	0.1456	0.1843	0.2318
	I	0.2841	0.4932	0.8110	1.0308
	R^2	0.9155	0.9106	0.8893	0.8694
Langmuir	k_L $(min)^{-1}$	0.0084	0.0085	0.0088	0.0107
	a	0.7343	0.7022	0.6783	0.5801
	R^2	0.9989	0.9988	0.9988	0.9993
Fractal-Langmuir	f	0.2804	0.2304	0.2827	0.2225
	n	0.8155	0.8175	0.8064	0.8325
	k_{FL} $(min)^{-\alpha}$	0.03504	0.0340	0.0356	0.0329
	R^2	0.9996	0.9996	0.9992	0.9991

5-7. Fractal Like-integrated Kinetic Langmuir Model

Fractal like-integrated kinetic Langmuir model has been presented by a combination of the fractal-like approach and integrated kinetic Langmuir equation by Haerifar and Azizian [65]:

$$\frac{q}{q_e} = \frac{(1-e^{-k_{FL}t^n})}{(1-fe^{-k_{FL}t^n})} \quad (18)$$

where, n, k_{FL} and f are FLIKL equation constants.

The kinetic parameters and correlation coefficients (R^2) obtained by fitting of kinetic data are shown in Table 5. For the pseudo-first-order, pseudo-second-order, Elovich, MPFO and intraparticle diffusion models, the values of the coefficients are less than 0.990 (R^2< 0.990). This result indicates the agreement between experimental data and these models can be weak and these models are not proper to fit the experimental kinetic data. For IKL and FLIKL models, the predicted values agree well with the experimental values (R^2> 0.99). Therefore, these models are applicable for fitting the experimental kinetic data. Also, comparison of the R^2 values of the two kinetic models indicates that the FLIKL model with R^2 value of 0.9991-0.9996 is better than the IKL model; it reveals that adsorbent surface is heterogeneous and has fractal like adsorption. It confirms the result of the isothermal study.

6. Thermodynamic studies

The thermodynamic parameters, ΔG^o, ΔH^o, and ΔS^o can be determined by using Eqs. (19) and (20):

$$\Delta G^o = -RT\ln K_C \quad (19)$$

$$\ln K_C = -\frac{\Delta G^o}{RT} = \frac{\Delta S^o}{R} - \frac{\Delta H^o}{RT} \quad (20)$$

where, T is the temperature of solution in Kelvin, K_C is the dimensionless equilibrium constant and R is the gas constant (8.314 J mol^{-1} K^{-1}). The K_C was obtained as a dimensionless parameter by multiplying K_L (Langmuir constant) by 55.5 and then 1000 [66]. The values of thermodynamic parameters were calculated from the plot of $\ln K_C$ versus 1/T. These plots are presented for CV adsorption on natural zeolite and Merck activated carbon in Fig. 10 and the results of thermodynamic parameters are summarized in Table 6.

ΔG^o has negative values for CV adsorption onto zeolite, which reflects the spontaneity of the process and affinity of CV to zeolites. However, the negative value of ΔG^o increases by increasing of temperature, indicating the nature of CV exchange is proportional to the temperature. For natural zeolite, the low and positive value of enthalpy shows that CV adsorption on the adsorbent surface is a physical process and endothermic. Also, the ion exchange is endothermic because some energy must be supplied to CV as it undergoes dehydration to occupy the less accessible sites located in the cages of zeolite [67]. The positive value of ΔS^o shows the randomness increasing at the solution during the adsorption process. The entropy also shows the changes of ion hydration, which occurs during the ion exchange process. The low value of ΔS^o indicates no remarkable changes in entropy occur during the adsorption process. Usually, enthalpy changes of ion exchange reactions in zeolites are small [67].

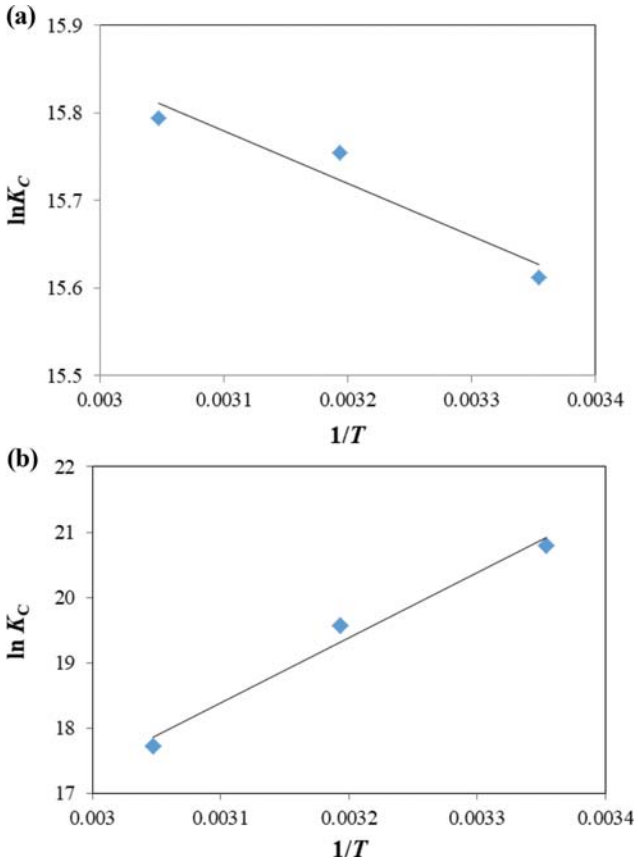

Fig. 10. The plot of $\ln K_C$ versus 1/T for CV adsorption on (a) natural zeolite and (b) Merck activated carbon.

ΔG^o has negative values for CV adsorption onto Merck carbon, which shows the adsorption process is spontaneous. In comparison to zeolite, the larger value of ΔG^o indicates more affinity of CV to activated carbon. Thermodynamic study for CV adsorption on Merck activated carbon shows this process is exothermic

Table 6. Thermodynamic parameters of dye adsorption on natural zeolite and Merck activated carbon

Adsorbent	Temperature (°C)	ΔG^o (kJ/mol)	ΔH^o (kJ/mol)	ΔS^o (kJ/mol K)
Natural zeolite	25	−38.715		
	40	−40.936	+4.979	+0.1466
	55	−43.136		
Merck activated carbon	25	−51.865		
	40	−50.283	−82.983	−0.104
	55	−48.717		

and the high value of enthalpy shows that it is a chemical process. It indicates the strong chemical bonding between CV and activated carbon occurs during adsorption. The negative value of ΔS^o shows the randomness decreasing during the adsorption process.

The results of enthalpy and entropy changing of CV adsorption on zeolite and activated carbon are different. This difference indicates the mechanisms of CV adsorption on these adsorbents are not the same. In the case of zeolite, ion exchange occurs, while CV only adsorbs on the surface activated carbon.

CONCLUSION

Natural zeolite as a low cost adsorbent has been used for removal of crystal violet from water. Modeling and optimizing of adsorption performance were performed by response surface methodology. Three effective variables were investigated and RSM results revealed the adsorbate-to-adsorbent weight ratio (%) is the most important variable, and it has negative effect on the dye removal. The results of ANOVA analysis, R^2 values and also lack of fit indicated that the model used in this study is proper. The optimum conditions were obtained at 0.1 g/g of adsorbate-to-adsorbent weight ratio, temperature=25 °C and pH=10. Various isotherms were applied to study CV adsorption on natural zeolite and activated carbon from Merck company. Among these isotherms, the Freundlich and Sips were the best for CV adsorption on zeolite and Merck activated carbon, respectively. Kinetic studies for natural zeolite indicated that the Fractal-Langmuir model is a suitable model. The thermodynamic parameters showed CV adsorption on natural zeolite is an endothermic and spontaneous process. The maximum adsorption capacities of natural zeolite, Merck activated carbon and different adsorbents for CV removal were compared. Results revealed that the zeolite used possesses the highest adsorption capacity (177.75 mg/g), and also it is an abundant and effective adsorbent for CV removal from wastewater.

ACKNOWLEDGEMENT

The authors are grateful to University of Kashan for supporting this work by Grant No. (682211/2).

REFERENCES

1. O. J. Hao, H. Kim and P. C. Chiang, *Environ. Sci. Technol.*, **30**, 449 (2000).
2. S. Li, *Bioresour. Technol.*, **101**, 2197 (2010).
3. S. Senthilkumaar, P. Kalaamani and C. V. Subburaam, *J. Hazard. Mater.*, **136**, 800 (2006).
4. H. He, S. Yang, K. Yu, Y. Ju and C. S. L. Wang, *J. Hazard. Mater.*, **173**, 393 (2010).
5. L. Guz, G. Curutchet, R. M. Torres Sánchez and R. Candal, *J. Environ. Chem. Eng.*, **2**, 2344 (2014).
6. H. Bashiri and M. Rafiee, *J. Saudi Chem. Soc.*, **20**, 474 (2016).
7. R. Zhu, Q. Chen, H. Liu, F. Ge, L. Zhu, J. Zhu and H. He, *Appl. Clay Sci.*, **88**, 33 (2014).
8. S. Eris and H. Bashiri, *Prog. React. Kinet. Mechanism*, **41**, 109 (2016).
9. S. V. K. Gupta, *Environ. Manage.*, **90**, 2313 (2009).
10. K. Banerjee, P. N.Cheremisinoff and S. L. Cheng, *Water Res.*, **31**, 249 (1997).
11. K. Y. Hor, J. M. C. Chee, M. N. Chong, B. Jin, C. Saint, P. E. Poh and R. Aryal, *J. Cleaner Prod.*, **118**, 197 (2016).
12. T. Sismanoglu, Y. Kismir and S. Karakus, *J. Hazard. Mater.*, **184**, 164 (2010).
13. I. Humelnicu, A. Băiceanu, M.-E. Ignat and V. Dulman, *Process Saf. Environ. Prot.*, **105**, 274 (2017).
14. M. Qiu, C. Qian, J. Xu, J. Wu and G. Wang, *Desalination*, **243**, 286 (2009).
15. R. P. Townsend, Chapter 10 Ion Exchange in Zeolites, in: H. van Bekkum, E. M. Flanigen, J. C. Jansen (Eds.) *Studies in Surface Science and Catalysis*, Elsevier, 359 (1991).
16. P. M. Pereira, B. F. Ferreira, N. P. Oliveira, E. J. Nassar, K. J. Ciuffi, M. A. Vicente, R. Trujillano, V. Rives, A. Gil, S. Korili and E. H. De Faria, *Appl. Sci.*, **8**, 608 (2018).
17. H. Awala, E. Leite, L. Saint-Marcel, G. Clet, R. Retoux, I. Naydenova and S. Mintova, *New J. Chem.*, **40**, 4277 (2016).
18. L. Campbell, A. Chimedtsogzol and A. Dyer, *Mineralogical Magazine*, **70**, 361 (2006).
19. L. S. Campbell, J. Charnock, A. Dyer, S. Hillier, S. Chenery, F. Stoppa, C. M. B. Henderson, R. Walcott and M. Rumsey, *Mineralogical Magazine*, **80**, 781 (2018).
20. C. A. Başar, *J. Hazard. Mater.*, **135**, 232 (2006).
21. A.-A. Peláez-Cid, A.-M. Herrera-González, M. Salazar-Villanueva and A. Bautista-Hernández, *J. Environ. Manage.*, **181**, 269 (2016).
22. S. Azizian, M. Haerifar and H. Bashiri, *Chem. Eng. J.*, **146**, 36 (2009).
23. C. Djilani, R. Zaghdoudi, F. Djazi, B. Bouchekima, A. Lallam, A. Modarressi and M. Rogalski, *J. Taiwan Inst. Chem. Engineers*, **53**, 112 (2015).
24. K. D. Belaid, S. Kacha, M. Kameche and Z. Derriche, *J. Environ. Chem. Eng.*, **1**, 496 (2013).
25. D. A. Giannakoudakis, G. Z. Kyzas, A. Avranas and N. K. Lazaridis, *J. Mol. Liq.*, **213**, 381 (2016).
26. Ö. Yavuz and A. H. Aydin, *Polish J. Environ. Studies*, **15**, 155 (2006).
27. S. M. Mousavi, D. Salari, A. Niaei, P. Nakhostin Panahi and S. Shafiei, *Environ. Technol.*, **35**, 581 (2014).
28. S. M. Mousavi and P. N. Panahi, *J. Taiwan Inst. Chem. Eng.*, **69**, 68 (2016).
29. Sh. Karimifard and M. R. Alavi Moghaddam, *Process Saf. Environ. Prot.*, **99**, 20 (2016).
30. M. K. Satapathy and P. Das, *J. Environ. Chem. Eng.*, **2**, 708 (2014).
31. A. Asfaram, M. Ghaedi, A. Goudarzi and M. Rajabi, *Dalton Trans.*, **44**, 14707 (2015).
32. V. Hernández-Montoya, M. A. Pérez-Cruz, D. I. Mendoza-Castillo, M. R. Moreno-Virgen and A. Bonilla-Petriciolet, *J. Environ. Manage.*, **116**, 213 (2013).
33. N. S. Flores-López, J. Castro-Rosas, R. Ramírez-Bon, A. Mendoza-Córdova, E. Larios-Rodríguez and M. Flores-Acosta, *J. Mol. Struct.*, **1028**, 110 (2012).
34. E. A. Dila, M. Ghaedi and A. Asfaram, *Ultrason. Sonochem.*, **34**, 792 (2017).
35. Y. Xue, H. Hou and S. Zhu, *Chem. Eng. J.*, **147**, 272 (2009).
36. N. Danesh, M. Hosseini, M. Ghorbani and A. Marjani, *Synth. Met.*, **220**, 508 (2016).
37. I. Langmuir, *J. Am. Chem. Soci.*, **38**, 2221 (1916).

38. H. Freundlich, *Zeitschrift für Physikalische Chemie*, **57U**, 385 (1907).
39. M. J. Temkin and V. Pyzhev, *Acta Physicochimica U.R.S.S.*, **12**, 327 (1940).
40. J. Febrianto, A. N. Kosasih, J. Sunarso, Y.-H. Ju, N. Indraswati and S. Ismadji, *J. Hazard. Mater.*, **162**, 616 (2009).
41. G. Alberti, V. Amendola, M. Pesavento and R. Biesuz, *Coord. Chem. Rev.*, **256**, 28 (2012).
42. K. Y. Foo and B. H. Hameed, *Chem. Eng. J.*, **156**, 2 (2010).
43. H. Bashiri and S. Eris, *Chem. Eng. Commun.*, **203**, 628 (2016).
44. A. M. K. P. Singh, S. Sinha and P. Ojha, *J. Hazard. Mater.*, **150**, 626 (2008).
45. T. C. R. Bertolini, J. C. Izidoro, C. P. Magdalena and D. A. Fungaro, *Orbital: Electron. J. Chem.*, **5**, 179 (2013).
46. E. A. Dila, M. Ghaedi, A. Ghaedi, A. Asfaram, M. Jamshidi and M. K. Purkai, *J. Taiwan Inst. Chem. Eng.*, **59**, 210 (2015).
47. O. S. Amodu, T. V. Ojumu, S. K. Ntwampe and O. S. Ayanda, *J. Encapsulation Adsorpt. Sci.*, **5**, 191 (2015).
48. S. Senthilkumaar, P. Kalaamani and C. V. Subburaam, *J. Hazard. Mater.*, **136**, 800 (2006).
49. B. K. Nandi, A. Goswami, A. K. Das, B. Mondal and M. K. Purkait, *Sep. Sci. Technol.*, **43**, 1382 (2008).
50. H. Yang, D. Zhou, Z. Chang and L. Zhang, *Desalin. Water Treat.*, **52**, 6113 (2014).
51. T. S. Anirudhan, P. S. Suchithra and P. G. Radhakrishnan, *Appl. Clay Sci.*, **43**, 336 (2009).
52. Z. Chen, T. Wang, X. Jin, Z. Chen, M. Megharaj and R. Naidu, *J. Colloid Interface Sci.*, **398**, 59 (2013).
53. S. Hamidzadeh, M. Torabbeigi and S. J. Shahtaheri, *J. Environ. Health Sci. Eng.*, **13**, 8 (2015).
54. P. Rai, R. K. Gautam, S. Banerjee, V. Rawat and M. C. Chattopadhyaya, *J. Environ. Chem. Eng.*, **3**, 2281 (2015).
55. J. P. Simonin, *Chem. Eng. J.*, **300**, 254 (2016).
56. S. Lagergren, *Kungliga Svenska Vetenskapsakademiens. Handlingar*, **24**, 1 (1898).
57. Y. L. Kang, S. K. S. Toh, P. Monash, S. Ibrahim and P. Saravanan, *Asia-Pacific J. Chem. Eng.*, **8**, 811 (2013).
58. S. Çoruh, F. Geyikçi and O. Nuri Ergun, *Environ. Technol.*, **32**, 1183 (2011).
59. X. Yang and B. Al-Duri, *J. Colloid Interface Sci.*, **287**, 25 (2005).
60. S. Azizian and H. Bashiri, *Langmuir*, **24**, 11669 (2008).
61. S. Azizian, *J. Colloid Interface Sci.*, **276**, 47 (2004).
62. H. Bashiri and A. Hassani Javanmardi, *Chem. Phys. Lett.*, **671**, 1 (2017).
63. H. Bashiri, *Chem. Phys. Lett.*, **575**, 101 (2013).
64. A. W. Marczewski, *Langmuir*, **26**, 15229 (2010).
65. M. Haerifar and S. Azizian, *J. Phys. Chem. C*, **116**, 13111 (2012).
66. H. N. Tran, S.-J. You and H.-P. Chao, *J. Environ. Chem. Eng.*, **4**, 2671 (2016).
67. L. Tagami, O. Santos, E. F. Sousa-Aguiar, P. A. Arroyo and M. Barros, *Acta Scientiarum*, **23**, 1351 (2001).
68. M. Ishaq, F. Javed, I. Amad and H. Ullah, *J. Chem. Chem. Eng.*, **35**, 97 (2016).